19A.5 RAPID-SCAN DUAL-POLARIZATION RADAR OBSERVATIONS OF Z_{DR} COLUMN DEPTH IN THE CONTEXT OF FORECASTER CONCEPTUAL MODELS

Charles M. Kuster*[1,2,3], Jeffrey C. Snyder[1,2,3], Pamela L. Heinselman[2,3], and Terry J. Schuur[1,2,3]

[1]Cooperative Institute for Mesoscale Meteorological Studies, [2]NOAA/OAR National Severe Storms Laboratory, [3]University of Oklahoma, Norman, Oklahoma

ABSTRACT

National Weather Service forecasters apply scientific conceptual models during warning operations to anticipate changes in storm intensity and associated hazards. Dual-polarization radar signatures such as Z_{DR} columns may provide additional insights about storm intensity and evolution, especially when integrated into these existing forecaster conceptual models. Increases in volumetric radar update time may also improve forecaster ability to observe changes in important radar signatures. Therefore, a research Weather Surveillance Radar-1988 Doppler radar located in Norman, Oklahoma was used to collect 15 rapid-scan dual-polarization cases (1.6–2.1 min volumetric updates) of tornadic, nontornadic, and nonsevere thunderstorms to compare Z_{DR} column depth evolution with signatures forecasters frequently use during warning operations (e.g., upper-level reflectivity cores; mesocyclones). An analysis of 7 cases to date has revealed that 1) peaks in Z_{DR} column depth size occur about 12 min prior to peaks in -20°C reflectivity core size, 2) peaks in Z_{DR} column depth size occur about 13 min prior to severe hail/wind reports, 3) consistent trends in Z_{DR} column depth size and magnitude were not observed prior to tornadogenesis, and 4) rapid-update volumetric radar data is likely beneficial for sampling short-lived (i.e., 10 min or less) trends and patterns in Z_{DR} column depth. In the future, once all cases are analyzed, a statistical analysis will be used to identify any operationally-relevant relationships between Z_{DR} column depth, -20°C reflectivity cores, mesocyclones, and storm reports, as well as quantifying typical Z_{DR} column depth size and magnitude for a wide variety of storm modes and intensities in Oklahoma.

---

1. INTRODUCTION

The dual-polarization (dual-pol) upgrade of the Weather Surveillance Radar-1988 Doppler (WSR-88D) radar network in 2013 gives National Weather Service (NWS) forecasters access to additional radar data that may aid them during severe weather events (NOAA 2013). Recent radar-based and numerical weather prediction studies have consistently observed several signatures commonly associated with supercells such as the differential reflectivity (Z_{DR}) arc, Z_{DR} ring, and specific differential phase (K_{DP}) foot (e.g., Kumjian and Ryzhkov 2008; Romine et al. 2008; Crowe et al. 2010; Mahale et al. 2012). Characteristics of these signatures and their evolution may also provide additional information about the potential hazards of a storm. For example, Crowe et al. (2012) noted spatial separation of the Z_{DR} arc and K_{DP} foot while storms were producing tornadoes, while Mahale et al. (2012) found that maximum Z_{DR} values within the Z_{DR} arc increased as vortex rotational velocities increased within quasi-linear convective systems.

A dual-pol signature that could be especially useful to NWS forecasters is the Z_{DR} column because it has been linked to updraft location and intensity (e.g., Hall et al. 1984; Ryzhkov et al. 1994; Kumjian et al. 2014; Snyder et al. 2015). Specifically, Kumjian et al. (2014) produced numerical simulations of Z_{DR} columns and found a strong correlation between the maximum height of the 2-dB Z_{DR} isosurface and the vertical velocity (i.e., updraft strength) at that height. A large and tall Z_{DR} column is therefore likely indicative of a strong updraft, which can be associated with hazards such as heavy rain, hail, lightning, and increasing low-level vorticity (e.g., Picca et al. 2010; Kumjian et al. 2012, 2014, Snyder et al. 2015). With this potential connection between Z_{DR} columns and storm hazards, Z_{DR} column evolution may be useful to NWS forecasters for short-term prediction of storm intensity and potential threats.

Radar based studies such as Picca et al. (2010, 2015) and Van Den Broeke (2017) have examined

Corresponding author address: Charles M. Kuster, National Weather Center, 120 David L. Boren Blvd., Norman, OK, 73072. E-mail: charles.kuster@noaa.gov

many supercells to assess operationally-relevant characteristics and trends of Z_{DR} columns. Picca et al. (2010) noted that an increase in Z_{DR} column depth preceded an increase in near-surface reflectivity by about 15–25 min while Picca et al. (2015) found that Z_{DR} column depth tends to decrease somewhat (400–600 m) prior to the development of significant tornadoes. In addition, Van Den Broeke (2017) noted that the Z_{DR} columns of supercells that produced significant tornadoes were taller and about 70% larger than the Z_{DR} columns of supercells that produced weak tornadoes. The research efforts however, did not find any distinguishable differences between the Z_{DR} columns of tornadic and nontornadic supercells or an appreciable decrease in Z_{DR} column depth prior to tornadogenesis.

Previous work has also identified some knowledge gaps relative to Z_{DR} columns and their use during NWS warning operations. Kumjian and Ryzhkov (2008) and Kuster and Heinselman (2015) highlighted the need to identify dual-pol precursors to tornadogenesis, which could increase forecaster confidence in issuing a tornado warning. Picca et al. (2015) performed a large analysis of Z_{DR} column depth evolution in supercells, but only measured maximum Z_{DR} column depth and stressed a need for statistical analysis of the Z_{DR} column. Picca et al. (2015) also noted that dual-pol signature evolution should be examined using rapid-scan volumetric radar data, while Van Den Broeke et al. (2008) and Picca et al. (2015) pointed towards a need for analysis of Z_{DR} columns within nontornadic supercells.

Therefore, the purpose of this research is to assess operational utility of Z_{DR} column depth evolution for multiple storm types and severities by using rapid-scan volumetric radar data to link dual-pol signature evolution to the evolution of signatures typically used by NWS forecasters to issue severe weather warnings (e.g., upper-level reflectivity cores; mesocyclones). Output from the Z_{DR} column depth algorithm (Snyder et al. 2015) is used to calculate evolution of median Z_{DR} column depth and size over time relative to the evolution of the -20°C reflectivity core and mesocyclone and the timing of severe-weather reports. Fifteen rapid-scan cases containing 32 supercells—20 of which are nontornadic—and 15 multi or single-cell thunderstorms have been identified for analysis. This paper will focus on the initial observations and findings from an analysis of 7 of these cases that contain 23 storms. An in depth qualitative and statistical analysis will follow once analysis has been completed for all cases.

RADAR DATA AND CASE INFORMATION

Rapid-scan volumetric radar data was collected using a research WSR-88D located in Norman, OK (KOUN). KOUN transmits at a wavelength of 11.09 cm (S-band), has an effective beamwidth of 1.06°, and can be operated in a system test mode that enables specialized operations for research purposes. Specifically, radar operators can perform 90° sector scans and unique volume coverage patters (VCP)—typically containing fewer elevation angles than standard WSR-88D VCPs—to collect volume scans with update times typically between 1.2 and 2.1 min. The seven cases analyzed so far occurred between 2013 and 2017 and include tornadic, nontornadic, and nonsevere thunderstorms (Table 1).

Two algorithms were run on KOUN data to produce information about Z_{DR} column depth and reflectivity values at -20°C. The Z_{DR} column depth algorithm (Snyder et al. 2015) produces a filtered three-dimensional field of Z_{DR} on a grid with spacing of 0.0025° in latitude and longitude and 250 m in the vertical. The algorithm then uses height of the environmental 0°C level from the Rapid Refresh (RAP) model (Brown et al. 2011) and the number of vertically consecutive grids with Z_{DR} of 1 dB or higher above the 0°C level to output a gridded product showing Z_{DR} column depth above 0°C (Fig. 1). The w2merger algorithm contained within the Warning Decision Support System-Integrated Information software (Lakshmanan et al. 2007) also uses RAP data to produce a gridded reflectivity field at -20°C, which was used to quantify the evolution of each storm's upper-level reflectivity core.

3. RADAR DATA ANALYSIS AND RESULTS

To quantify Z_{DR} column depth evolution, we manually extracted values output by the Z_{DR} column depth algorithm for each storm's Z_{DR} column and then calculated column depth magnitude and size. For magnitude, we calculated the median for all grids with a depth of 1000 m or higher and we approximated size by counting the number of grids with a depth of 1000 m or higher (Fig. 1). Magnitude and size of the -20°C reflectivity core was determined by calculating the median reflectivity and counting the number of grids that had reflectivity of 50 dBZ or higher. To quantify mesocyclone intensity evolution, we calculated the velocity difference (delta V) across the rotational signature at the elevation angle with an altitude closest to three km above radar level (ARL).

Table 1: Basic storm and radar information for all seven cases included in the analysis.

Date	**Storm Mode**	**Hazard Type**	**VCP Elevation Angles (°)**	**Update Time (min)**
27 April 2013	Nontornadic supercells; multicells	Hail/wind	0.52, 0.97, 1.5, 2.05, 3.05, 4.05, 5.05, 5.95, 7.97, 9.90	1.2–1.4
19 May 2013	Tornadic/nontornadic supercells	Tornado; hail/wind	0.52, 0.97, 1.5, 2.05, 3.05, 4.05, 5.05, 5.95, 7.97, 9.90	1.2–1.4
8 July 2014	Multicells	Hail/wind	0.30, 1.25, 2.20, 3.15, 4.10, 5.05, 6.00, 6.95, 7.90, 8.85, 9.80, 12.00, 14.00, 16.70	2.0
6 May 2015	Tornadic/nontornadic supercells	Tornado	VCP1: 0.50, 1.20, 1.80, 2.40, 3.00, 3.60, 4.20, 5.50, 7.70, 10.00 VCP2: 0.50, 1.50, 2.80, 3.90, 5.00, 6.10, 7.20, 8.40, 10.50, 13.00	1.4–1.6
16 May 2015	Tornadic supercell; multicell	Tornado; wind	0.50, 1.20, 1.80, 2.40, 3.00, 3.60, 4.20, 5.50, 7.70, 10.00	1.5
9 May 2016	Tornadic/nontornadic supercells	Tornado; hail	VCP1: 0.5, 0.9, 1.4, 2.4, 3.5, 4.6, 5.7, 7.1, 9.1, 11.4 VCP2: 0.5, 0.9, 1.4, 2.4, 3.5, 4.6, 5.7, 7.1, 9.1, 11.4 VCP3: 0.5, 0.9, 1.4, 1.8, 2.2, 2.7, 3.2, 3.9, 4.7, 5.6	1.5–1.9
26 March 2017	Tornadic/nontornadic supercells	Tornado, hail	VCP1: 0.5, 0.9, 1.4, 2.4, 3.5, 4.6, 5.7, 7.1, 9.1, 11.4 VCP2: 0.5, 0.9, 1.4, 2.0, 2.7, 3.5, 4.4, 5.5, 6.5, 7.7	1.5

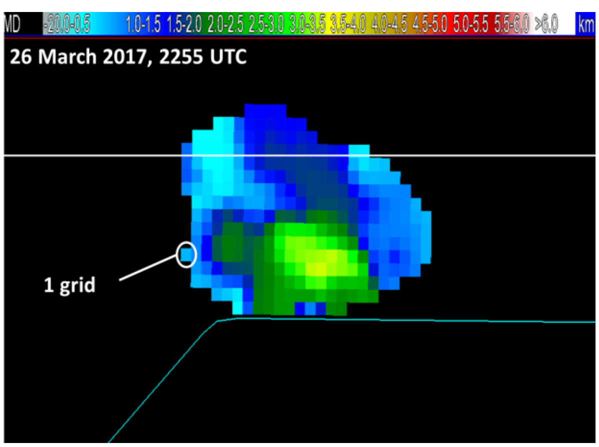

Fig. 1. Example output from the Z_{DR} column depth algorithm for a supercell on 26 March 2017. Colors show depth of Z_{DR} column above 0°C with warmer colors indicating greater depths. An individual lat/lon grid is highlighted.

3.1 Z_{DR} COLUMN DEPTH AND -20°C REFLECTIVITY CORES

In 14 of the 23 storms analyzed so far, peaks in Z_{DR} column depth size occurred on average about 12 min prior to peaks in -20°C reflectivity core size. Similar trends were also observed for signature magnitude (i.e., median Z_{DR} column depth), but were less pronounced and less common than those observed for signature size, so here we primarily focus on signature size. One clear example of this evolution occurred with a tornadic supercell that occurred on 9 May 2016 (Fig. 2a). In this event, Z_{DR} column depth size peaked at about 2156 UTC, while -20°C reflectivity core size peaked 14 min later at about 2210 UTC. This evolution holds for other storm types as well and was observed clearly for a nonsevere multicell thunderstorm on 8 July 2014 where a peak in Z_{DR} column depth size occurred 27 min (2254 UTC) prior to the primary peak in -20°C reflectivity core size (2321 UTC; Fig. 2b).

We did not observe this pattern for every storm, however. Four storms contained no clear relationship between Z_{DR} column depth size and -20°C reflectivity core size evolution, while the peak in -20°C reflectivity core size occurred before the peak in Z_{DR} column depth size in one storm. The other four storms had bad or incomplete data and were not included in the analysis. This difference in trends will be addressed with the future statistical analysis of all cases to determine if this pattern is commonly observed and therefore potentially beneficial to operational meteorologists.

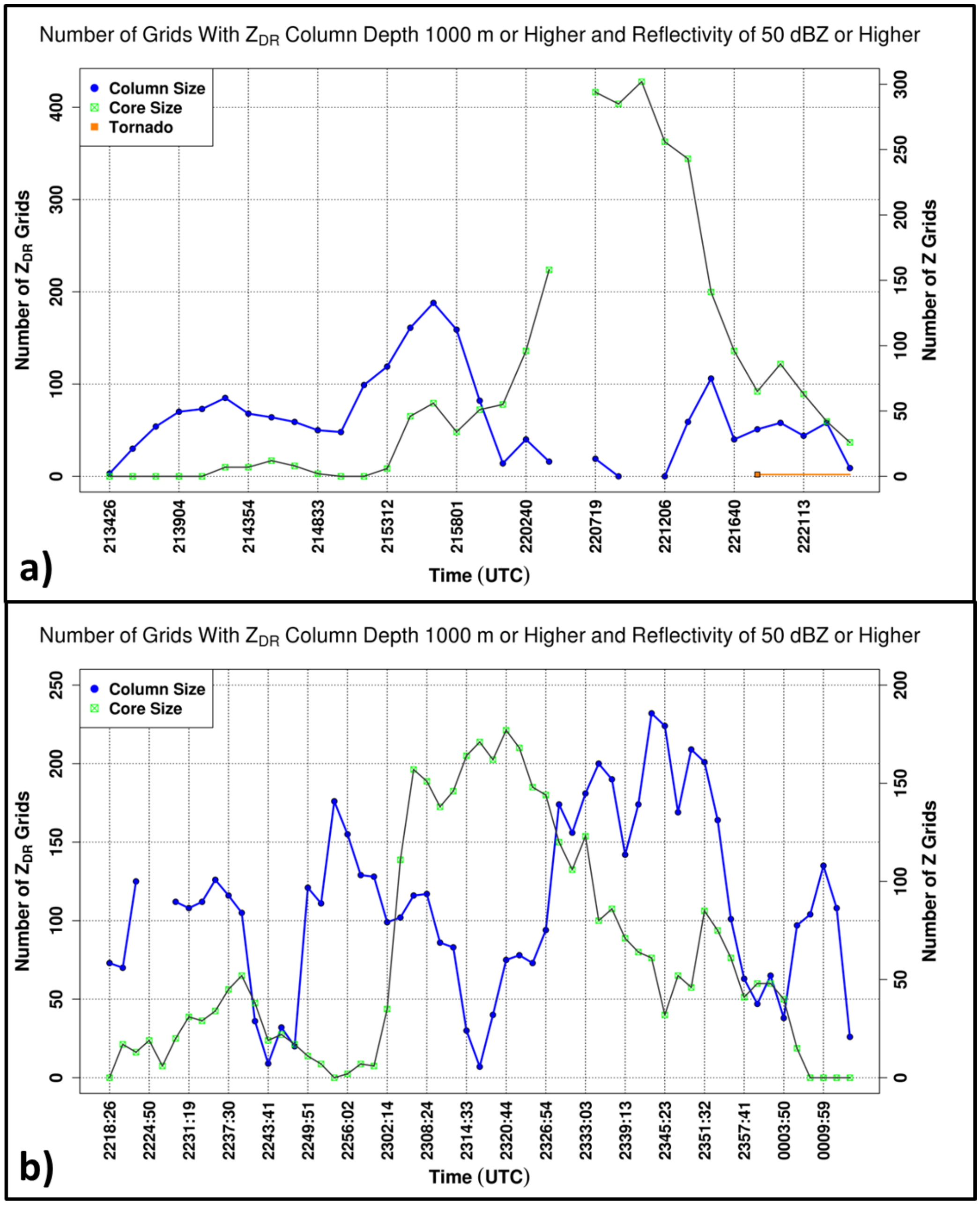

Fig. 2. Z_{DR} column depth size (blue line) and -20°C reflectivity core size (black line with green markers) for a storm on a) 9 May 2016 and b) 8 July 2014. The horizontal orange line in a) indicates when a tornado was ongoing.

3.2 Z_{DR} COLUMN DEPTH AND SEVERE HAIL/WIND REPORTS

The pattern of Z_{DR} column depth size and magnitude peaking prior to the peak in -20°C reflectivity core size described above could have operational significance, because these peaks frequently preceded severe-weather reports. For 19 of the 21 severe reports considered, a peak in Z_{DR} column depth size occurred on average about 13 min prior to a report. Considering trends could allow for additional precursor lead time, since Z_{DR} column depth size began increasing to its peak on average 17 min prior to a report. The precursor lead time did vary from 1 to 28 min for peak Z_{DR} column depth size and 5 to 34 min for increasing Z_{DR} column depth size, and two severe reports were not preceded by a peak in Z_{DR} column depth size. Therefore, the degree of operational benefits could differ on a case-by-case basis. For example, on 8 July 2014, a peak in Z_{DR} column depth size preceded all four severe reports by at least 12 min (Fig. 3a), but on 19 May 2013, a peak in Z_{DR} column depth size only preceded the hail report by 6 min and no peak occurred prior to the wind report (Fig. 3b).

The 8 July 2014 event also shows the potential for false alarms associated with peaks in Z_{DR} column depth size. The final peak in Z_{DR} column depth size that occurred at about 2357 UTC was not associated with any severe weather reports despite it having a similar magnitude and longer duration than the previous peak that was associated with 3 severe reports (Fig. 3a). There are limitations with Storm Data, however (e.g., Hales 1993; Trapp et al. 2006), so we cannot be certain that the storm did not produce any severe weather after 2340 UTC. There may have been severe weather but it was not reported or experienced by anyone. This limitation could affect the results of this study and alternative verification methods such as the Maximum Estimated Size of Hail algorithm (e.g., Witt et al. 1998; Cintineo et al. 2012) will be considered during future work.

3.3 Z_{DR} COLUMN DEPTH AND TORNADO DEVELOPMENT

Z_{DR} column depth evolution relative to tornado development and mesocyclone evolution was less consistent than that observed relative to severe hail and wind reports. Similarly to Picca et al. (2015), we did note a decreasing trend in Z_{DR} column depth size and magnitude prior to the development of 8 out of 12 tornadic mesocyclones considered. Z_{DR} column depth size and magnitude either increased (n=2) or displayed no trend (n=2) prior to the development of the other 4 tornadic mesocyclones considered. The two instances of increasing Z_{DR} column depth size and magnitude were associated with significant tornadoes (EF2+).

Z_{DR} column depth trends did not always remain constant and even reversed sign by the time tornadogenesis occurred for three tornadic mesocyclones. This trend reversal was most clear for a tornadic supercell that occurred on 19 May 2013. Z_{DR} column depth size decreased notably from 24 min to 8 min prior to tornadogenesis (2323:35–2338:42 UTC), but then began increasing 7 min prior to tornadogenesis and continued increasing through the 2-min duration of the tornado (Fig. 4a). We also observed decreasing Z_{DR} column depth size prior to the development of 6 out of 11 nontornadic mesocyclones considered, which can be most clearly seen for a nontornadic supercell on 27 April 2013 (Fig. 4b). It is possible that decreasing Z_{DR} column depth size is somewhat more common prior to the development of tornadic mesocyclones, but this pattern as well as pattern magnitudes will be examined in more depth once all cases are completed to identify characteristics (if any) that might aid forecasters in diagnosing a mesocyclone's tornadic potential.

3.4 POTENTIAL IMPACT OF RADAR UPDATE TIME

While not explicitly studied to date, it is probable that radar update time will have an impact on a forecaster's ability to observe the aforementioned trends and peaks in Z_{DR} column depth size and magnitude. In many instances, Z_{DR} column depth trends evolved over time scales of 10 min or less. Radars collecting rapid-scan volumetric data could sample a trend occurring over 10 min as many as 10 times, while the WSR-88D network may only sample the same trend twice. Analysis of a tornadic supercell on 9 May 2016 presents one example of this possibility. Between 2150:06 and 2201:07 UTC, Z_{DR} column depth size increased to a peak and then decreased to nearly zero in only 11 min (Fig. 2a, 5). KOUN sampled this evolution 8 times and provided a relatively clear picture of what occurred. By degrading the KOUN data to have a temporal resolution similar to the WSR-88D network for this case (6-min volumes), we were able to observe that a radar with slower radar updates might only sample this evolution twice (Fig. 5). It would therefore likely be more challenging for a forecaster to interpret signature evolution and utilize such information to positively impact a potential warning decision if only 6-min volumes were available. Future work will include direct comparisons of KOUN and WSR-88D data to quantify the impact of radar update time on sampling trends in Z_{DR} column depth across a wide variety of storm types.

4. RELEVANCE TO OPERATIONS

Scientifically based conceptual models provide a framework for NWS forecasters to effectively anticipate a storm's evolution and threats (Andra et al. 2002). Integration of new radar signatures (e.g., Z_{DR} column) into existing forecaster conceptual models will likely increase the utility of these signatures to forecasters during warning operations. This study therefore aims to identify operationally-relevant trends in Z_{DR} column depth and link those trends to radar signatures that forecasters already use to issue warnings (e.g., upper-level reflectivity cores; mesocyclones). Our initial observations suggest that Z_{DR} column depth size evolution is connected with upper-level

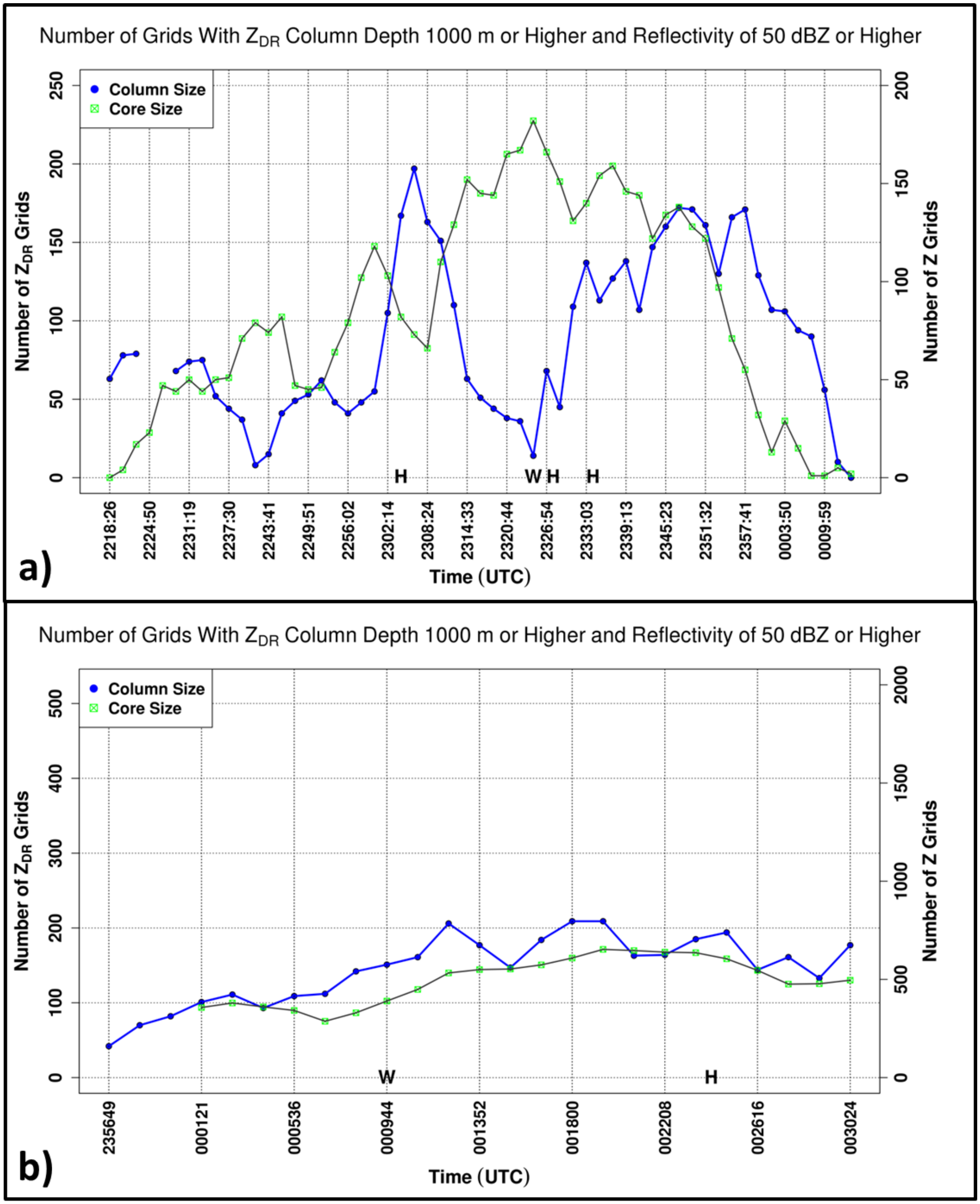

Fig. 3. Z_{DR} column depth size (blue line) and -20°C reflectivity core size (black line with green markers) for a storm on a) 8 July 2014 and b) 19 May 2013. **H** indicates the time of a severe hail report and **W** indicates the time of a severe wind report.

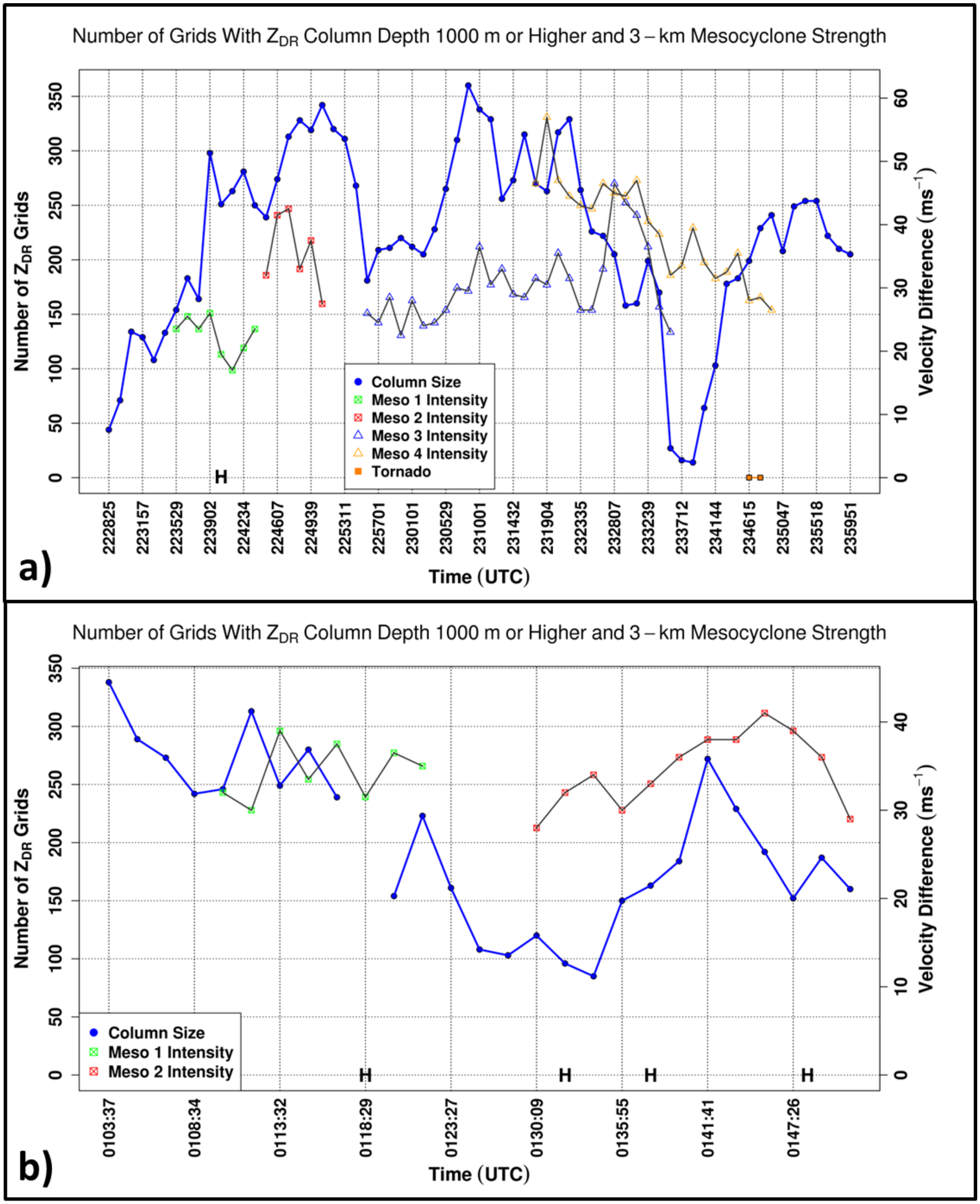

Fig. 4. Z_{DR} column depth size (blue line) and velocity difference measured across each mesocyclone at 3 km ARL (black lines with colored markers) for a) a tornadic storm on 19 May 2013 and b) a nontornadic storm on 27 April 2013. The horizontal line in a) indicates when a tornado was ongoing. **H** indicates the time of a severe hail report.

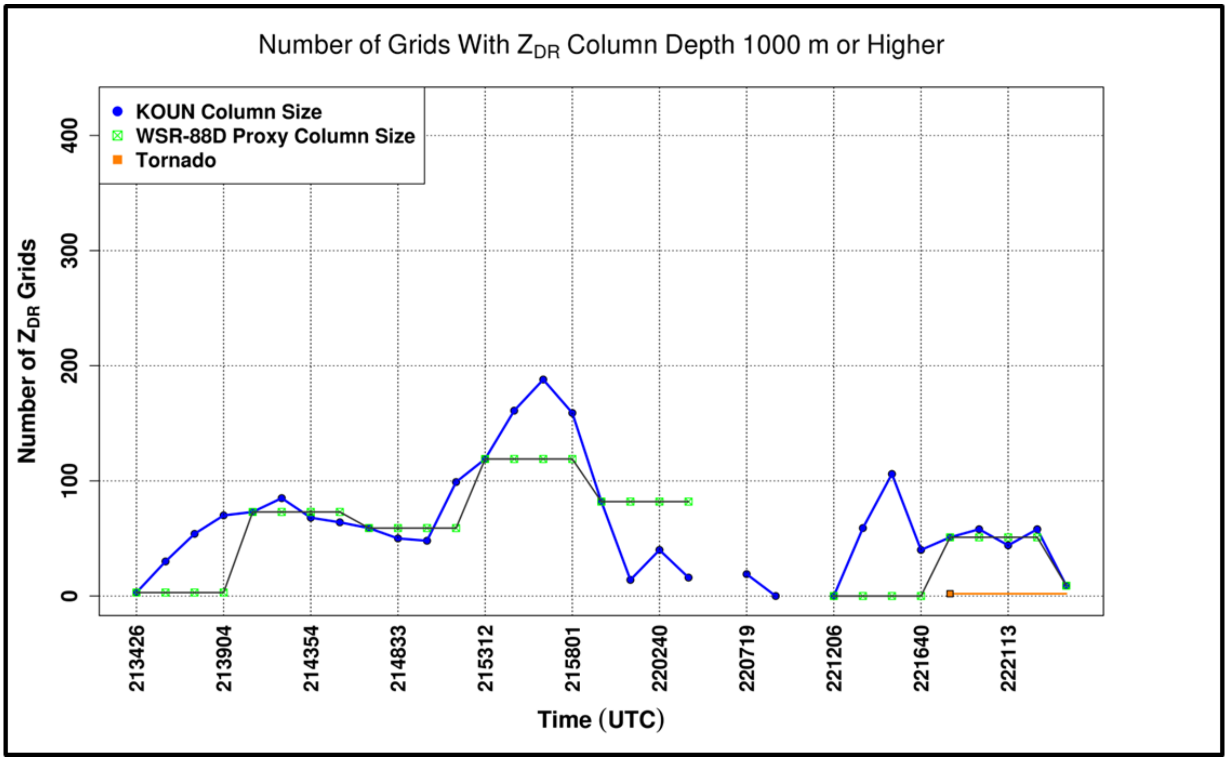

Fig. 5. Z_{DR} column depth size as sampled by KOUN rapid-scan data (blue line) and degraded KOUN data to match 6-min volume scan update times of a nearby WSR-88D radar (black line with green markers) for a storm on 9 May 2016. The horizontal orange line indicates when a tornado was ongoing.

reflectivity core evolution. Z_{DR} column depth size reached a peak prior to the peak in -20°C reflectivity core size for more than half of the storms considered. This observation is not surprising because Z_{DR} columns develop below the -20°C height and columns can develop after only a few large drops are carried above the environmental melting layer (e.g., Kumjian et al. 2014; Snyder et al. 2015). As an updraft accelerates upward, it will loft large drops above the melting layer (i.e., Z_{DR} column formation) before many hydrometeors develop and are suspended at higher altitudes (i.e., -20°C reflectivity core formation). This connection is likely important to forecasters because we frequently observed severe weather reports after peaks in Z_{DR} column depth size and -20°C reflectivity core size (Section 3.2). The development of a deep Z_{DR} column could alert a forecaster to severe weather potential before a strong upper-level reflectivity core develops, thereby alerting them that a given storm is intensifying and potentially allow them to issue a warning earlier. While the observed trends in Z_{DR} column depth do not appear to be a definitive precursor to severe hail and wind, this signature can likely provide forecasters with another piece of information that can help build confidence in issuing a severe thunderstorm warning.

Based on our results so far, integrating Z_{DR} column depth into forecaster conceptual models of tornadogenesis might be more challenging since no consistent relationship was observed between Z_{DR} column depth and mesocyclone evolution or tornado reports. In some cases Z_{DR} column depth size and magnitude decreased prior to tornadogenesis, while in other cases it increased. We also observed increasing Z_{DR} column depth prior to the development of two significant tornadoes (EF2+) and did not observe a clear difference in column depth between storms that produced significant tornadoes, weak tornadoes, or no tornadoes. These results differ from Picca et al. (2015) and Van Den Broeke (2017), perhaps because our sample size is currently much smaller than those studies. Connections between Z_{DR} column depth and mesocyclone evolution will continue to be examined and quantified as we complete analysis of all available rapid-scan cases.

Previous studies have identified operational benefits of using rapid-scan volumetric radar data for issuing severe thunderstorm and tornado warnings (e.g., Heinselman et al. 2012; Wilson et al. 2017). Based on the cases analyzed so far, we expect rapid-scan volumetric radar data will allow for more effective sampling of short-lived changes in Z_{DR} column depth. The ability to observe these changes will likely help forecasters identify threatening storms sooner and allow them to provide additional information to their partners and the general public with potentially longer lead times. Any technique that would decrease the volumetric update time of the WSR-88D network would likely be beneficial for observing Z_{DR} columns as well as other deep signatures (e.g., upper-level reflectivity cores, midlevel mesocyclones).

SUMMARY AND FUTURE WORK

The research presented here is part of a larger ongoing study of 15 rapid-scan datasets containing Z_{DR} column depth evolution for severe and nonsevere thunderstorms. Through analysis of the first 7 cases, we have observed trends that might be relevant to NWS forecasters, especially those that relate to the evolution of upper-level reflectivity cores and storm reports (Section 3.1 and 3.2). In these cases, Z_{DR} column depth size peaks about 12 min prior to -20°C reflectivity core size on average and increasing Z_{DR} column depth size occurs about 17 min prior to severe weather reports on average. Peaks in Z_{DR} column depth size do occur without severe weather reports, however (Fig. 2b, 3), and we did not observe a clear consistent connection with mesocyclone evolution or tornado reports. These uncertainties will be addressed when all cases are completed and a comprehensive statistical and qualitative analysis is performed. With this analysis we aim to determine if the trends observed in the first seven cases are representative across all cases and if there are any consistent relationships between Z_{DR} column depth, -20°C reflectivity, and mesocyclone evolution that might prove useful to forecasters issuing warnings.

We will also use the larger analysis to comment on typical Z_{DR} column depth size and magnitude for a variety of storm modes and intensities in Oklahoma. This information could help forecasters know when to begin paying attention to a storm and when a warning might be needed based on Z_{DR} column depth evolution. In addition, an analysis of Z_{DR} column depth, -20°C reflectivity cores, and mesocyclone evolution will be completed using data from a nearby WSR-88D (KTLX). A direct comparison of radars with different volumetric update times will allow for an evaluation of radar update time's impact on observing and using Z_{DR} column depth for nowcasting purposes.

Acknowledgements. We thank Jeff Brogden, John Krause, Karen Cooper and Robert Toomey for their help with WDSS-II, three forecasters at the NWS Norman Forecast Office (Doug Speheger, Randy Bowers, and Vivek Mahale) for input on operational storm interrogation practices, and Katie Wilson for insight into the forecaster warning decision making process. Funding for CK, JS, and TS was provided by NOAA/Office of Oceanic and Atmospheric Research under NOAA-University of Oklahoma Cooperative Agreement #NA11OAR4320072, U.S. Department of Commerce.

REFERENCES

Andra, D. L., E. M. Quoetone, and W. F. Bunting, 2002: Warning decision making: The relative roles of conceptual models, technology, strategy, and forecaster expertise on 3 May 1999. *Wea. Forecasting*, **17**, 559–566.

Brown, J. M., and Coauthors, 2011: Improvement and testing of WRF physics options for application to Rapid Refresh and High Resolution Rapid Refresh. Proc. *14th Conf. on Mesoscale Processes/15th Conf. on Aviation, Range, and Aerospace Meteorology*, Los Angeles, CA, Amer. Meteor. Soc., 5.5. [Available online at https://ams.confex.com/ams/ 14Meso15ARAM/webprogram/Paper191234.html.]

Cintineo, J. L., T. M. Smith, V. Lakshmanan, H. E. Brooks, and K. L. Ortega, 2012: An objective high-resolution hail climatology of the contiguous United States. *Wea. Forecasting*, **27**, 1235–1248.

Crowe, C. C., C. J. Schultz, M. Kumjian, L. D. Carey, and W. A. Petersen, 2012: Use of dual-polarization signatures in diagnosing tornadic potential. *Electronic J. Operational Meteor.*, **13**, 57–78.

Hales, J. E., Jr., 1993: Biases in the severe thunderstorm data base: Ramifications and solutions. Preprints, *13th Conf. on Weather Forecasting and Analysis*, Vienna, VA, Amer. Meteor. Soc. 504–507.

Hall, M. P. M., J. W. F. Goddard, and S. M. Cherry, 1984: Identification of hydrometeors and other targets by dual-polarization radar. *Radio Sci.*, **19**, 132–140.

Heinselman, P. L., D. S. LaDue, and H. Lazrus, 2012: Exploring impacts of rapid-scan radar data on NWS warning decisions. *Wea. Forecasting*, **27**, 1031–1044.

NOAA, 2013: Dual-polarization radar: Stepping stones to building a Weather-Ready Nation. Accessed 30 September 2015. [Available online at http://www.nws.noaa.gov/com/weatherreadynation/news/130425_dualpol.html#.VhaC3Le-1f5].

Kumjian, M. R., and A. V. Ryzhkov, 2008: Polarimetric signatures in supercell thunderstorms. *J. Appl. Meteor. Climatol.*, **47**, 1940–1961.

——, S. M. Ganson, and A. V. Ryzhkov, 2012: Freezing in deep convective updrafts: A microphysical and polarimetric model. *J. Atmos. Sci.*, **69**, 3471–3490.

——, A. P. Khain, N. Benmoshe, E. Ilotoviz, A. V. Ryzhkov, and V. T. J. Phillips, 2014: The anatomy and physics of Z_{DR} columns: Investigating a polarimetric radar signature with a spectral bin microphysical model. *J. Appl. Meteor. Climatol.*, **53**, 1820–1843.

Kuster, C. M., and P. L. Heinselman, 2015: Rapid-scan, dual-polarization radar observations of tornadic and nontornadic mesocyclones in the context of forecaster conceptual models. *Extended Abstracts, 37th Conf. on Radar Meteorology*, Norman, OK, Amer. Meteor. Soc., 4A.2. [Available online at https://ams.confex.com/ams/37RADAR/webprogram/Paper274991.html].

Lakshmanan, V., T. Smoth, G. J. Stumpf, and K. Hondl, 2007: The Warning Decision Support System–Integrated Information. *Wea. Forecasting*, **22**, 596–612.

Mahale, V. N., J. A. Brotzge, and H. B. Bluestein, 2012: An analysis of vorticies embedded within a quasi-linear convective system using X-band polarimetric radar. *Wea. Forecasting*, **27**, 1520–1537.

Picca, J. C., M. Kumjian, and A. V. Ryzhkov, 2010: Z_{DR} columns as a predictive tool for hail growth and storm evolution. *Extended Abstracts, 25th Conf. on Severe Local Storms*, Denver, CO, Amer. Meteor. Soc., 11.3 [Available online at https://ams.confex.com/ams/pdfpapers/175750.pdf].

——, J. C. Snyder, and A. V. Ryzhkov, 2015: An observational analysis of Z_{DR} column trends in tornadic supercells. *Extended Abstracts, 37th Conf. on Radar Meteorology*, Norman, OK, Amer. Meteor. Soc., 5A.5. [Available online at https://ams.confex.com/ams/37RADAR/webprogram/Paper275416.html].

Romine, G. S., D. W. Burgess, and R. B. Wilhelmson, 2008: A dual-polarization-radar-based assessment of the 8 May 2003 Oklahoma City area tornadic supercell. *Mon. Wea. Rev.*, **136**, 2849–2870.

Ryzhkov, A. V., V. B. Zhuravlyov, and N. A. Rybakova, 1994: Preliminary results of X-band polarization radar studies of clouds and precipitation. *J. Atmos. Oceanic Technol.*, **11**, 132–139.

Snyder, J. C., A. V. Ryzhkov, M. R. Kumjian, A. P. Khain, and J. Picca, 2015: A Z_{DR} column detection algorithm to examine convective storm updrafts. *Wea. Forecasting*, **30**, 1819–1844.

Trapp, R. J., D. M. Wheatley, N. T. Atkins, R. W. Przbylinski, and R. Wolf, 2006: Buyer beware: Some words of caution on the use of severe wind reports in postevent assessment and research. *Wea. Forecasting*, **21**, 408–415.

Van Den Broeke, M. S., 2017: Polarimetric radar metrics related to tornado life cycles and intensity in supercell storms. *Mon. Wea. Rev.*, **145**, 3671–3686.

——, M. S., J. M. Straka, and E. N. Rasmussen, 2008: Polarimetric radar observations at low levels during tornado life cycles in a small sample of classic southern plains supercells. *J. Appl. Meteor. Climatol.*, **47**, 1232–1247.

Witt, A., M. D. Eilts, G. S. Stumpf, J. T. Johnson, E. D. Mitchell, and K. W. Thomas, 1998: An enhanced hail detection algorithm for the WSR-88D. *Wea. Forecasting*, **13**, 286–303.

Wilson, K. A., P. L. Heinselman, C. M. Kuster, D. M. Kingfield, and Z. Khang, 2017: Forecaster performance and workload: Does radar update time matter? *Wea. Forecasting*, **32**, 253–274.